Key Points:
- One second averages of the chorus waves at the equator are correlated with 1 s average microburst electron precipitation
- The 1 s averaged microburst flux is consistent with the quasi-linear diffusion of equatorial electrons by the equatorial chorus wave
- Quasi-linear diffusion cannot explain the faster (~0.2 s) microburst flux variations caused by the large amplitude (~1 nT) chorus waves

Simultaneous Observations of Lower Band Chorus Emissions at the Equator and Microburst Precipitating Electrons in the Ionosphere

F. S. Mozer[1], O. V. Agapitov[1], J. B. Blake[2] [ID], and I. Y. Vasko[1]

[1]Space Sciences Laboratory, University of California, Berkeley, CA, USA, [2]Space Science Applications Laboratory, The Aerospace Corporation, El Segundo, CA, USA

Abstract On 11 December 2016 at 00:12:30 UT, Van Allen Probe-B, at the equator and near midnight, and AC6-B, in the ionosphere, were on magnetic field lines whose 100 km altitude foot points were separated by 600 km. Van Allen Probe-B observed a 30 s burst of lower band chorus waves (with maximum amplitudes >1 nT) at the same time that AC6-B observed intense microburst electrons in the loss cone. One second averaged variations of the chorus intensity and the microburst electron flux were well correlated. The low-altitude electron flux expected from quasi-linear diffusion of the equatorial electrons by the equatorial chorus is in excellent agreement with the observed, 1 s averaged, low-altitude electron flux. However, the large-amplitude, <0.5 s duration, low-altitude electron pulses require nonlinear processes for their explanation.

1. Introduction

Microbursts are the impulsive precipitation of 30 keV to 1 MeV electrons from the radiation belts into the atmosphere on time scales of a few tenths of a second. They were first measured by Anderson and Milton (1964) on X-ray balloons, and they have since been observed on many balloons, rockets and satellites (Datta et al., 1996; Dietrich et al., 2010; Douma et al., 2017; Imhof et al., 1992; Lampton, 1967; Millan et al., 2002; Millan & the Barrel Team, 2011; O'Brien et al., 2004; Parks, 1974, 1978; Parks et al., 1979). Early on, their occurrence was associated with chorus emissions at the equator (Chang & Inan, 1983; Kersten et al., 2011; Lam et al., 2010; Lorentzen et al., 2001; Ni, Bortnik, et al., 2014; Oliven & Gurnett, 1968; Rosenberg et al., 1981, 1990; Skoug et al., 1996; Thorne, 2010, Thorne et al., 2013). The precipitation of >30 keV electrons observed by low-altitude Polar Operational Environmental Satellites spacecraft have been used to evaluate the intensity of chorus waves at the equator (Li et al., 2013; Ni, Li, et al., 2014).

In this paper, we present the first conjunction along a magnetic field line of lower band chorus waves at the equator and ionospheric precipitating microburst electrons. The equatorial measurements were made on the Van Allen Probes (Blake et al., 2013; Kletzing et al., 2013; Wygant et al., 2013), while the ionospheric electron flux in the loss cone was measured by the AC6-B satellite (Blake & O'Brien, 2016). We demonstrate that the flux of precipitating electrons observed by AC6 and averaged over 1 s is in agreement with the prediction from quasi-linear theory although the more rapid flux variations require a nonlinear interaction.

2. Data

On 11 December 2016, at 00:12:30 UT, Van Allen Probe B was located at 6 R_e geocentric altitude near midnight on a magnetic field line whose foot point, at an altitude of 100 km, was located at 67.4° latitude and 345.5° longitude. At the same time, the AC6-B satellite was in the ionosphere on a field line whose 100 km foot point was at 62.3° latitude and 347.7° longitude. The separation of the foot points at 100 km over the event was about 600 ± 100 km. AC6-B measured electrons >35 keV that were in the local loss cone, while Van Allen Probe-B observed chorus waves. Figure 1 displays 0.1 s averages of the electron flux measured by AC6-B and the magnitude of the perpendicular magnetic field in the chorus wave (the component of the wave field that is perpendicular to the background magnetic field) measured on Van Allen Probe-B. The temporal correlation between the equatorial chorus wave and the loss cone electrons strongly suggests that the chorus wave caused the bursty electron precipitation. The same microburst structure was observed in the northern ionosphere within a few minutes of the AC6 measurement by NOAA15 and MET02, and at the
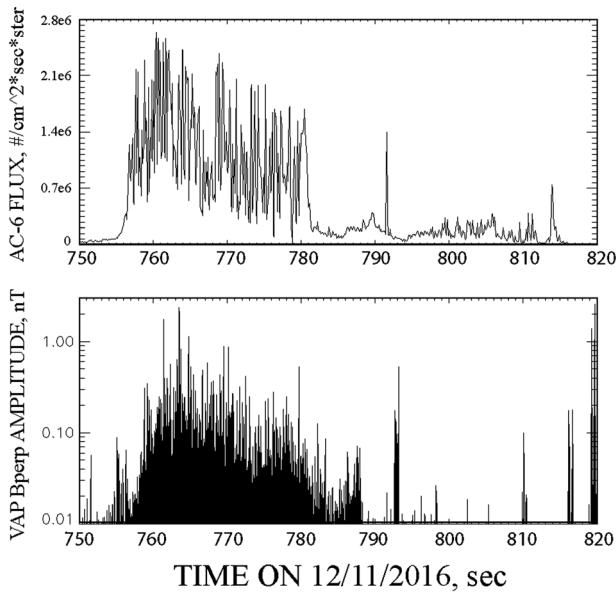
Figure 1. The top panel gives the 0.1 s averaged >35 keV precipitating electron counting rate observed on the AC6-B satellite in the ionosphere, while the bottom panel gives the amplitude of the perpendicular magnetic field observed at the equator on a field line that maps to the vicinity of the AC6-B satellite.

conjugate point in the southern hemisphere by NOAA18. The satellite foot point separations from AC6 of these three spacecraft varied from 500 to 5,000 km. This shows that the precipitation was wide spread (Agapitov et al., 2017), which adds further support to the conclusion that the observed equatorial chorus wave produced the microburst.

An expanded example of the AC6-B electron counting rate and the Van Allen Probe-B chorus wave is given in Figure 2. Both parameters showed fast (~0.2 s) large-amplitude fluctuations that were similar in their temporal variations but that did not correlate in detail. These rapid fluctuations qualify this event as being a long duration microburst. It is noted that the AC6-B flux varied by as much as a factor of 4 in less than 0.2 s.

A 20 ms snapshot of the unfiltered chorus electric and magnetic field waveforms, as obtained from the raw time series, is given in Figure 3. Along with Figure 1, this demonstrates that the chorus magnetic field was sometimes >1 nT, an extremely large value. As indicated by this data and Figure 2c, chorus was the only wave present during the entire event. Its central frequency was about 1,800 Hz, which is about 35% of the electron gyrofrequency, while its frequency width was about 500 Hz.

Figure 4 (left) gives a scatter plot of the 1 s averaged, normalized electron flux and the similarly normalized perpendicular magnetic field in the chorus wave. The dashed curve is a polynomial least squares fit to the scatterplot data. The colored curves come from the quasi-linear calculation of the precipitation expected from the equatorial data that is discussed below.

Figure 4 (right) gives the correlation between the equatorial wave and the ionospheric electrons as a function of lag time. For a lag near zero, the correlation is greater than 0.8, a very high value for two such independent measurements. Although the precipitation should occur a fraction of a second after the chorus wave, the sign of the maximum lag suggests that the precipitation occurred before the chorus waves. This just indicates that the Van Allen Probes entered the equatorial region occupied by the chorus waves about 1 s after the AC6 measurements of the electrons scattered out of this region. In summary, these data provide convincing evidence that the chorus waves produced equatorial electron scattering that resulted in a large electron microburst precipitating into the upper atmosphere.
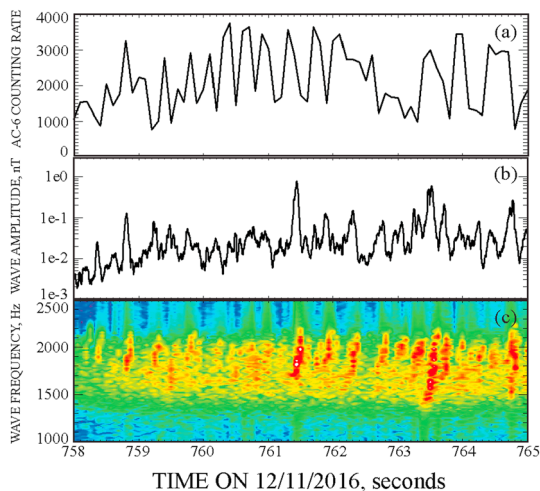

Figure 2. Example of the rapid flux variations observed (a) in the precipitating electrons and (b) in the chorus wave amplitude at the equator. (c) The wavelet spectrum of the chorus magnetic field.

3. Quasi-Linear Estimates

A first-order estimate of the flux within the loss cone expected from scattering of the equatorial electrons by the equatorial chorus can be obtained using quasi-linear theory. To compute the flux within the loss cone, one needs estimates of the electron flux near the loss cone and the bounce-averaged pitch angle scattering rate driven by the chorus waves at the loss cone boundary (e.g., Kennel, 1969). The electron fluxes near the loss cone $j(E, \alpha_{LC})$ are estimated using Van Allen Probe measurements near the equator, as shown in Figure 5b, although the loss cone is not resolved. The total flux of electrons with energies $E > E_{th}$ within the loss cone is

$$\Phi(E_{th}) = \pi \int_{E_{th}}^{\infty} x(E)\, j(E, \alpha_{LC}) dE \qquad (1)$$

where $x(E) = 2\, I_0^{-1}(z_0) \int_0^1 I_0(z_0 \tau)\, \tau\, d\tau$, $z_0(E) = \left(D_{SD}/D_{\alpha\alpha}|_{\alpha=\alpha_{LC}} \right)^{1/2}$ and I_0 is the modified Bessel function. The parameter, $x(E)$, takes into account the fact that the electron flux within the loss cone generally differed from the flux at the loss cone boundary, and it depends on the ratio between
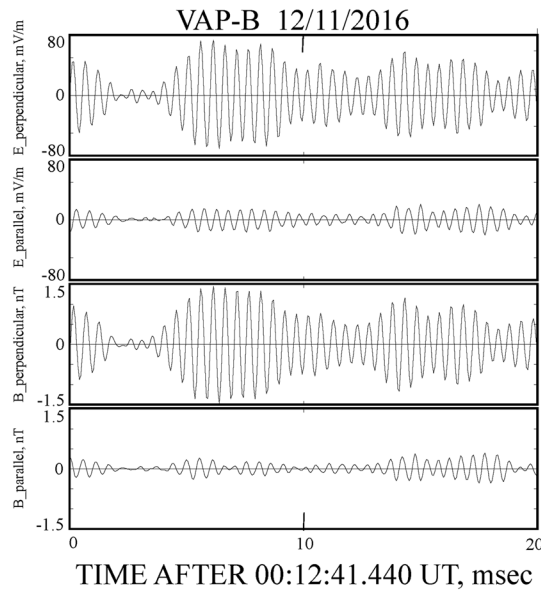
VAP-B 12/11/2016

TIME AFTER 00:12:41.440 UT, msec

Figure 3. The perpendicular and parallel components of (first and second panels) the electric field and (third and fourth panels) magnetic field in the chorus wave observed at the equator. It is noted that no other wave activity was present.

the diffusion coefficient at the loss cone boundary, $D_{\alpha\alpha}|_{\alpha=\alpha_{LC}}$, and the strong diffusion coefficient, $D_{SD} = \alpha_{LC}^2/T_B(E)$. T_B is one quarter of the bounce period, which depends on the electron energy E (e.g., Kennel, 1969; Ni et al., 2012). In the strong diffusion regime, $D_{\alpha\alpha}|_{\alpha=\alpha_{LC}} > D_{SD}$, the loss cone is full and $x(E) = 1$, while in the case of weak diffusion, the loss cone is only partially filled and $x(E) < 1$. To evaluate the total flux within the loss cone, one needs to compute the quasi-linear bounce-averaged pitch angle diffusion coefficient $D_{\alpha\alpha}$ at the loss cone boundary. The energy of the electrons scattered by the chorus wave is strongly dependent on the background plasma density and background magnetic field. The measured density of >200 eV electrons was 0.3 cm^{-3} at the time of the microburst. Extrapolating to lower energies suggests that the total electron density was 1–2 cm^{-3}. The three densities 0.5, 1.0 and 2.0 cm^{-3} were used to compute the quasi-linear pitch angle diffusion coefficients, while the background magnetic field was assumed to be a dipole.

We restrict our estimates to parallel chorus waves (because the observed waves had wave normal angles <10°, as seen by the ratio of the magnetic fields in Figure 3, third and fourth panels), and we compute the quasi-linear pitch angle diffusion coefficient following Summers (2005). The chorus properties are adopted from the Van Allen Probe measurements presented, for example, in Figure 3. We have verified that the magnetic field power spectral density of the chorus waves is well fitted by the expression $I_B(f) = A \exp[-(f - f_0)^2/\delta f^2]$, where $f_0 = 1780$ Hz, $\delta f = 230$ Hz and the frequency range is $|f - f_0| < 2\delta f$. The parameter, A, is related to the root-mean-square (RMS) chorus wave intensity B_w^2 by the standard relations (e.g., Summers, 2005). In computing the bounce-averaged diffusion coefficients we assumed that the plasma density was constant along the equatorial magnetic field line and that the chorus waves were concentrated at latitudes <30°, in agreement with statistical studies (Agapitov et al., 2015; Meredith et al., 2012), where the power spectral density and the RMS intensity are independent of latitude. The pitch angle diffusion coefficients near the loss cone computed for 100 pT chorus waves are presented in Figure 5a. The diffusion coefficient is greater than the strong diffusion limit over a limited range of electron energies that depend on the background plasma density (alternatively, on the ratio, f_{pe}/f_{ce}, the electron plasma frequency to the electron gyrofrequency). Due to the variation of the RMS chorus wave intensity B_w shown in Figure 1, the diffusion coefficient varies during the event. The time dependent
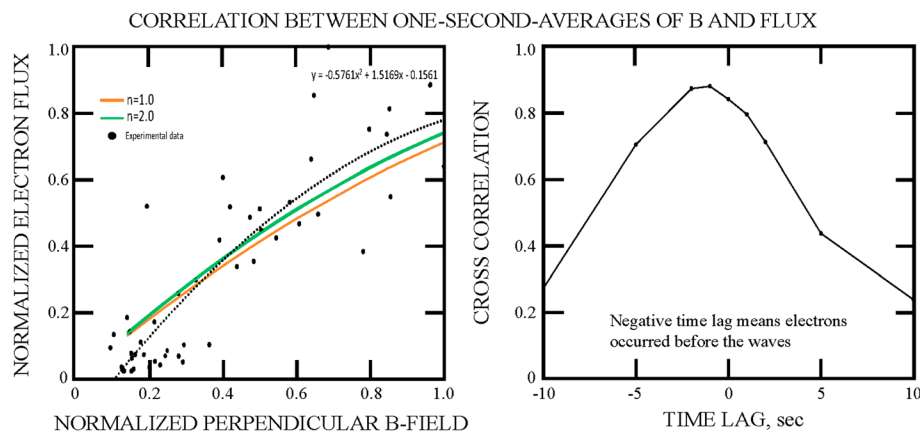

CORRELATION BETWEEN ONE-SECOND-AVERAGES OF B AND FLUX

Figure 4. Evidence that the equatorial wave and ionospheric electron precipitation were correlated. (left) A scatterplot of the 1 s averaged electron flux versus the 1 s averaged perpendicular magnetic field amplitude. The dashed curve is the polynomial least squares fit to the experimental data. The colored lines are the quasi-linear diffusion predictions for densities of 1.0, and 2.0 cm^{-3}, respectively. (right) The correlation between the electron flux and the wave as a function of lag time. The correlation maximizes at a value near 0.9 for a lag of about 1 s, with the chorus appearing at the equator after the electrons appear at the ionosphere.
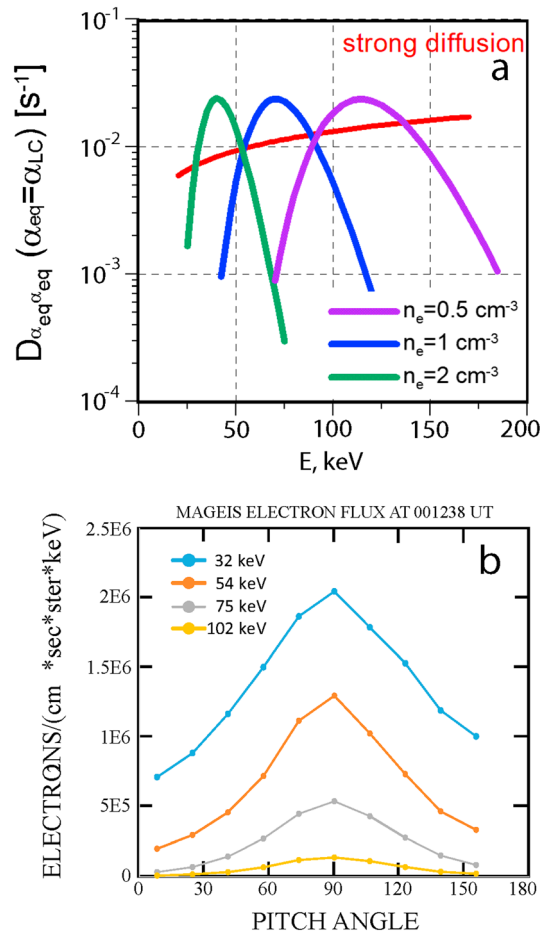
Figure 5. (a) Diffusion coefficients for different values of the plasma density. (b) The pitch angle distribution of electrons with four energies, measured at the VAP-B satellite during the event. In a quasi-linear diffusion model, the smallest pitch angle electrons diffuse into the loss cone to become the precipitating microburst.
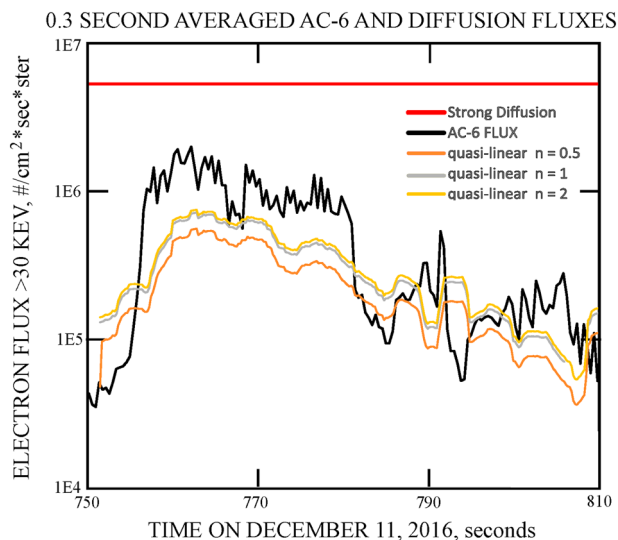

Figure 6. The observed electron flux versus time (black curve) along with the fluxes expected from strong diffusion (the red line) and from quasi-linear diffusion for different values of the plasma density (the other curves).

diffusion coefficient is used to compute the total flux of electrons in the loss cone with energies above the AC6 lower-energy threshold E_{th} that is about 35 keV. Since the diffusion is greater than strong diffusion in the limited energy range, the differential electron flux within the loss cone is generally nonuniform. AC6 measured the averaged electron flux over the full loss cone. Therefore, we evaluate the average differential flux within the loss cone from quasi-linear theory as $\Phi(E_{th})/2\pi$, which depends on time due to the varying RMS chorus wave intensity. In the computation, the diffusion coefficients are updated every second and compared to the 1 s average of the measured flux in Figures 4a and 6.

Estimates of the normalized (to the maximum amplitude of the flux measured by AC6) differential electron flux computed from quasi-linear diffusion for the different background plasma densities are presented versus the normalized wave magnetic field in Figure 4a. The excellent agreement between the calculated electron flux for densities of 1 or 2 cm^{-3} (the blue and red curves) and the least squares fit to the data (the dashed curve) shows that quasi-linear diffusion is appropriate for estimating the relative amplitude of the 1 s averaged microburst fluxes. The largest uncertainty in the quasi-linear flux calculation arises from the uncertainty of the plasma density.

Figure 6 presents the absolute differential electron flux measured by AC6 and the quasi-linear diffusion estimates. The red line is the differential flux expected for strong diffusion at all energies above the AC6 lower-energy threshold. The observed differential electron flux is in satisfactory agreement with the quasi-linear estimates. In this comparison of absolute fluxes, the largest uncertainty (the order of a factor of 3) is that due to the AC6 measurement because this detector did not have a well-defined entrance aperture and it did not measure a spectrum. (The AC6 detector was calibrated by comparison to measurements of precipitating and trapped electron fluxes at somewhat higher altitudes (Li et al., 2013; Ni, Li, et al., 2014)).

It is noted that the measured flux is clearly below the strong diffusion limit. This latter fact could also be anticipated from Figure 4a, which shows that the precipitating electron flux is proportional to the RMS chorus wave intensity. For strong diffusion at all energies, the electron flux would be independent of the chorus wave intensity.

4. Discussion

In this paper, we have presented a conjunction event between bursty electron precipitation observed by AC6 at low altitudes for a few tens of seconds and chorus waves observed by the Van Allen Probes at the equator. We have used the equatorial electron fluxes measured by the MAGEIS instrument and the root mean square (1 s averaged) chorus wave intensity to evaluate the flux of precipitating electrons, using quasi-linear theory. The predicted precipitating flux agrees very well with the normalized flux measured by AC6 and the absolute flux agrees within the factor of ~3 uncertainty of the measurement.

At the same time, the presented event draws attention to an important effect. The quasi-linear theory is in best agreement with the observed electron fluxes only after averaging the data over about 1 s. In fact, as shown in Figure 3, the flux significantly changes on a

time scale of a fraction of a second due to scattering by individual chorus elements. Although amplitudes of chorus elements are usually below 100 pT, there are chorus elements with amplitudes as high as 1 nT that are sufficient to make nonlinear effects in the resonant interaction significant (e.g., Tao et al., 2012). Therefore, it is unexpected that the quasi-linear theory provides a reasonable estimate of the 1 s averaged precipitating electron fluxes. Whether this implies that on a long time scale, nonlinear scattering looks like quasi-linear scattering will be addressed in future studies.

References

Agapitov, O. V., Artemyev, A. V., Mourenas, D., Mozer, F. S., & Krasnoselskikh, V. (2015). Empirical model of lower band chorus wave distribution in the outer radiation belt. *Journal of Geophysical Research: Space Physics*, *120*(12), 10,425–10,442. https://doi.org/10.1002/2015JA021829

Agapitov, O. V., Blum, L. W., Mozer, F. S., Bonnell, J. W., & Wygant, J. (2017). Chorus whistler wave source scales as determined from multipoint Van Allen Probe measurements. *Geophysical Research Letters*, *44*, 2634–2642. https://doi.org/10.1002/2017GL072701

Anderson, K. A., & Milton, D. W. (1964). Balloon observations of X-rays in the auroral zone. *Journal of Geophysical Research*, *69*(4457), 1964.

Blake, J. B., & O'Brien, T. P. (2016). Observations of small-scale latitudinal structure in energetic electron precipitation. *Journal of Geophysical Research: Space Physics*, *121*, 3031–3035. https://doi.org/10.1002/2015JA021815

Blake, J. B., Carranza, P. A., Claudepierre, S. G., Clemmons, J. H., Crain, W. R., Dotan, Y., … Zakrzewski, M. P. (2013). The magnetic electron ion spectrometer (MagEIS) instruments aboard the radiation belt storm probes (RBSP) spacecraft. *Space Science Reviews*, *179*(1-4), 383–421. https://doi.org/10.1007/s11214-013-9991-8

Chang, H. C., & Inan, U. S. (1983). A theoretical model study of observed correlations between whistler mode waves and energetic electron precipitation events in the magnetosphere. *Journal of Geophysical Research*, *88*(A12), 10053. https://doi.org/10.1029/JA088iA12p10053

Datta, S., Skoug, R. M., McCarthy, M. P., & Parks, G. K. (1996). Analysis and modeling of microburst precipitation. *Geophysical Research Letters*, *23*(14), 1729–1732. https://doi.org/10.1029/96GL01672

Dietrich, S., Rodger, C. J., Clilverd, M. A., Bortnik, J., & Raita, T. (2010). Relativistic microburst storm characteristics: Combined satellite and ground-based observations. *Journal of Geophysical Research*, *115*, A12240. https://doi.org/10.1029/2010JA015777

Douma, E., Rodger, C. J., Blum, L. W., & Clilverd, M. A. (2017). Occurrence characteristics of relativistic electron microbursts from SAMPEX observations. *Journal of Geophysical Research: Space Physics*, *122*, 8096–8107. https://doi.org/10.1002/2017JA024067

Imhof, W. L., Voss, H. D., Mobilia, J., Datlowe, D. W., Gaines, E. E., McGlennon, J. P., & Inan, U. S. (1992). Relativistic electron microbursts. *Journal of Geophysical Research*, *97*(A9), 13829. https://doi.org/10.1029/92JA01138

Kennel, C. F. (1969). Consequences of a magnetospheric plasma. *Reviews of Geophysics and Space Physics*, *7*(1, 2), 379–419. https://doi.org/10.1029/RG007i001p00379

Kersten, K., Cattell, C. A., Breneman, A., Goetz, K., Kellogg, P. J., Wygant, J. R., … Roth, I. (2011). Observation of relativistic electron microbursts in conjunction with intense radiation belt whistler-mode waves. *Geophysical Research Letters*, *38*, L08107. https://doi.org/10.1029/2011GL046810

Kletzing, C. A., Kurth, W. S., Acuna, M., MacDowall, R. J., Torbert, R. B., Averkamp, T., … Tyler, J. (2013). The Electric and Magnetic Field Instrument Suite and Integrated Science (EMFISIS) on RBSP. *Space Science Reviews*, *179*(1-4), 127–181. https://doi.org/10.1007/s11214-013-9993-6

Lam, M. M., Horne, R. B., Meredith, N. P., Glauert, S. A., Moffat-Griffin, T., & Green, J. C. (2010). Origin of energetic electron precipitation >30 keV into the atmosphere. *Journal of Geophysical Research*, *115*, A00F08. https://doi.org/10.1029/2009JA014619

Lampton, M. (1967). Daytime observations of energetic auroral-zone electrons. *Journal of Geophysical Research*, *72*(23), 5817–5823. https://doi.org/10.1029/JZ072i023p05817

Li, W., Ni, B., Thorne, R. M., Bortnik, J., Green, J. C., Kletzing, C. A., … Hospodarsky, G. B. (2013). Constructing the global distribution of chorus wave intensity using measurements of electrons by the POES satellites and waves by the Van Allen Probes. *Geophysical Research Letters*, *40*, 4526–4532. https://doi.org/10.1002/grl.50920

Lorentzen, K. R., Blake, J. B., Inan, U. S., & Bortnik, J. (2001). Observations of relativistic electron microbursts in association with VLF chorus. *Journal of Geophysical Research*, *106*(A4), 6017–6027. https://doi.org/10.1029/2000JA003018

Meredith, N. P., Horne, R. B., Sicard-Piet, A., Boscher, D., Yearby, K. H., Li, W., & Thorne, R. M. (2012). Global model of lower band and upper band chorus from multiple satellite observations. *Journal of Geophysical Research*, *117*, A10225. https://doi.org/10.1029/2012JA017978

Millan, R. M., & the Barrel Team (2011). Understanding relativistic electron losses with BARREL. *Journal of Atmospheric and Solar-Terrestrial Physics*, *73*(11-12), 1425–1434. https://doi.org/10.1016/j.jastp.2011.01.006

Millan, R. M., Lin, R. P., Smith, D. M., Lorentzen, K. R., & McCarthy, M. P. (2002). X-ray observations of MeV electron precipitation with a balloon-borne germanium spectrometer. *Geophysical Research Letters*, *29*(24), 47–41 2194.

Ni, B., Liang, J., Thorne, R. M., Angelopoulos, V., Horne, R. B., Kubyshkina, M., … Lummerzheim, D. (2012). Efficient diffuse auroral electron scattering by electrostatic electron cyclotron harmonic waves in the outer magnetosphere: A detailed case study. *Journal of Geophysical Research*, *117*, A01218. https://doi.org/10.1029/2011JA017095

Ni, B., Li, W., Thorne, R. M., Bortnik, J., Green, J. C., Kletzing, C. A., … de Soria-Santacruz Pich, M. (2014). A novel technique to construct the global distribution of whistler mode chorus wave intensity using low-altitude POES electron data. *Journal of Geophysical Research: Space Physics*, *119*, 5685–5699. https://doi.org/10.1002/2014JA019935

Ni, B., Bortnik, J., Nishimura, Y., Thorne, R. M., Li, W., Angelopoulos, V., … Weatherwax, A. T. (2014). Chorus wave scattering responsible for the Earth's dayside diffuse auroral precipitation: A detailed case study. *Journal of Geophysical Research: Space Physics*, *119*, 897–908. https://doi.org/10.1002/2013JA019507

O'Brien, T. P., Looper, M. D., & Blake, J. B. (2004). Quantification of relativistic electron microburst losses during the GEM storms. *Geophysical Research Letters*, *31*, L04802. https://doi.org/10.1029/2003GL018621

Oliven, M. N., & Gurnett, D. A. (1968). Microburst phenomena, 3. An association between microbursts and VLF chorus. *Journal of Geophysical Research*, *73*(7), 2355–2362. https://doi.org/10.1029/JA073i007p02355

Parks, G. K. (1974). Auroral zone microbursts, substructures, and a model for microburst precipitation, Proc. Int. Conf. on X-rays in Space, Calgery, Alberta, Canada, August 14-21 (pp. 849–874).

Parks, G. K. (1978). Microburst precipitation phenomena. *Journal of Geomagnetism and Geoelectricity*, *30*(4), 327–341. https://doi.org/10.5636/jgg.30.327

Parks, G. K., Gurgiolo, C., & West, R. (1979). Relativistic electron precipitation. *Geophysical Research Letters*, *6*(5), 393–396. https://doi.org/10.1029/GL006i005p00393

Rosenberg, T. J., Siren, J. C., Matthews, D. L., Marthinsen, K., Holtet, J. A., Egeland, A., … Helliwell, R. A. (1981). Conjugacy of electron microbursts and VLF chorus. *Journal of Geophysical Research*, *86*(A7), 5819. https://doi.org/10.1029/JA086iA07p05819

Rosenberg, T. J., Wei, R., Detrick, D. L., & Inan, U. S. (1990). Observations and modeling of wave-induced microburst electron precipitation. *Journal of Geophysical Research*, *95*(A5), 6467. https://doi.org/10.1029/JA095iA05p06467

Skoug, R. M., Datta, S., McCarthy, M. P., & Parks, G. K. (1996). A cyclotron resonance model of VLF chorus emissions detected during electron microburst precipitation. *Journal of Geophysical Research*, *101*(A10), 21,481–21,491. https://doi.org/10.1029/96JA02007

Summers, D. (2005). Quasi-linear diffusion coefficients for field-aligned electromagnetic waves with applications to the magnetosphere. *Journal of Geophysical Research*, *110*, A08213. https://doi.org/10.1029/2005JA011159

Tao, X., Bortnik, J., Albert, J. M., & Thorne, R. M. (2012). Comparison of bounce-averaged quasi-linear diffusion coefficients for parallel propagating whistler mode waves with test particle simulations. *Journal of Geophysical Research*, *117*, A10205. https://doi.org/10.1029/2012JA017931

Thorne, R. M. (2010). Radiation belt dynamics: The importance of wave-particle interactions. *Geophysical Research Letters*, *37*, L22107. https://doi.org/10.1029/2010GL044990

Thorne, R. M., Li, W., Ni, B., Ma, Q., Bortnik, J., Chen, L., … Kanekal, S. G. (2013). Rapid local acceleration of relativistic radiation-belt electrons by magnetospheric chorus. *Nature*, *504*(7480), 411–414. https://doi.org/10.1038/nature12889

Wygant, J. R., Bonnell, J. W., Goetz, K., Ergun, R. E., Mozer, F. S., Bale, S. D., … Tao, J. B. (2013). The Electric Field, and Waves (EFW) instruments on the Radiation Belt Storm Probes Mission. *Space Science Reviews*, *179*(1-4), 183–220. https://doi.org/10.1007/s11214-013-0013-7